NUCL SCI TECH (2019) 30:114
https://doi.org/10.1007/s41365-019-0630-2

Influence of copper element distribution and speciation on the color of Chinese underglaze copper-red porcelain in the Yuan dynasty

Mao-Lin Zhang[1] · Li-Hua Wang[2,3] · Li-Li Zhang[2,3] · Hai-Sheng Yu[3]

Received: 14 November 2018 / Revised: 20 February 2019 / Accepted: 20 March 2019 / Published online: 12 June 2019

Abstract A shard of Chinese underglaze copper-red porcelain from the Yuan dynasty (AD 1271–1368) made in the Jingdezhen kiln was measured by synchrotron radiation-induced X-ray fluorescence mapping and X-ray absorption near-edge spectroscopy to investigate the influence of copper element distribution and speciation on the color of porcelain. In black-colored region, copper accumulates at the interface between the body and glaze layers with metallic copper particles as the main speciation. In contrast, Cu is irregularly distributed in the red-colored region with multi-valence speciation. The differences in Cu distribution and speciation in black- and red-colored regions indicate that they are the main factors influencing the different colors of copper-red underglaze porcelain.

Keywords Copper distribution and speciation · Chinese underglaze copper-red porcelain · Synchrotron techniques

This work was supported by Natural Science Foundation of China (Nos. 51762027 and 11875312) and Jiangxi Collaborative Innovation Center of Ceramic Relics Conservation and Imperial Kiln Research.

Electronic supplementary material The online version of this article (https://doi.org/10.1007/s41365-019-0630-2) contains supplementary material, which is available to authorized users.

✉ Li-Hua Wang
lhwang@sinap.ac.cn

[1] Institute of Ancient Ceramics, Jingdezhen Ceramic Institute, Jingdezhen 333403, China

[2] Shanghai Synchrotron Radiation Facility, Shanghai Advanced Research Institute, Chinese Academy of Sciences, Shanghai 201210, China

[3] Shanghai Institute of Applied Physics, Chinese Academy of Sciences, Shanghai 201204, China

1 Introduction

Chinese underglaze copper-red porcelain usually designates white porcelains fired at high temperature and decorated with copper-based pigments between body and glaze. It was first developed at the Jingdezhen kiln in the Yuan dynasty (AD 1271–1368) with colors varying from red to black on the same item. During the Hongwu era (AD 1368–1398) of the Ming dynasty, most underglaze copper-red porcelain had a red color with gray hues. The technique of making this type of porcelain continued to improve till the Yongle era (AD 1403–1424) and Xuande era (AD 1426–1435) of the Ming dynasty; subsequently, a decline was observed in the middle and late eras of the Ming dynasty (AD 1435–1644). The development was revived again till the Kangxi era (AD 1622–1722) of the Qing dynasty [1]. Because copper is sensitive to the firing atmosphere and easily dissolves and diffuses in glaze, it is difficult to obtain the red color. Therefore, the color of copper-red underglaze porcelain is very unstable and varies from purple to red to gray to black and even disappears in some regions. Thus far, there are three possible factors that could impart the red color of Chinese underglaze copper-red porcelain. The first one is metallic copper particles. In 1936, J. W. Mellor first reported the finding that colloidal metallic copper particles were responsible for the red color [2]. This was confirmed by many researchers in copper-red glasses, glazes, and decorations [3–9]. Furthermore, Kingery and Vandiver [10] pointed out that colloidal metallic copper particles with sizes from several tens of nanometers to one micrometer contribute to the copper-red color. The second one factor is Cu_2O microcrystals, as reported by many researchers [11–14]. The third possibility is that both colloidal metallic copper particles and Cu_2O

microcrystals are responsible for the red color of copper-red glaze reported by Chinese ceramists, based on a substantial research and modeling experiments [3].

In contrast, only a few studies pay attention to the reason why underglaze copper-red porcelain exhibits different hues. Guan et al. [15] used the micro-synchrotron radiation-induced XRF technique to investigate the chemical compositions in different color areas in a shard of underglaze copper-red porcelain from the early Ming dynasty by line scanning. They found that the Cu concentration increased noticeably with the colors changing from gray to red; furthermore, the appearance of the color mainly depended on the amount of copper in the pigments. Another study by the same group confirmed that copper concentration in the red region was higher than that in the orange region in Yuan underglaze copper-red porcelain. They also found that the Cu speciation in both red and orange regions is metallic copper and the differences between red- and orange-colored regions originated from the Mie scatter effect [16]. Furthermore, the difference of Cu speciation in the red- and black-colored regions is also observed in Xuande sacrificial red porcelain from the Guan kiln of Jingdezhen [17]. It is necessary to study in detail the origin of different colors in a single piece of porcelain using comparative analysis including both Cu concentration and speciation for black and red colors.

Given that the glaze layer for copper-red underglaze porcelain is usually several hundred micrometers, the use of micro-beam analytical methods is required. Synchrotron-induced μ-X-ray fluorescence (μ-XRF) spectrometry and μ-X-ray absorption near-edge spectroscopy (μ-XANES) have been proven to be a powerful tool to investigate the speciation of elements in small regions of typically a few micrometers. This method has been applied widely in many scientific fields [18–27]. It provides the spatial distribution of elements and association with other elements by scanning the regions of interest in a regular grid pattern by the X-ray micro-beam and detecting the induced fluorescence intensities at each position. XANES spectroscopy could provide the chemical form of a certain element for materials having a complex composition and an amorphous phase. Therefore, the spatial distribution of elements and the chemical form of copper in underglaze copper-red porcelain have been investigated by the means of synchrotron radiation-induced μ-XRF and μ-XANES micro-spectroscopy. The basic purpose was to obtain the spatial distribution of copper, the association of copper with other elements, and the chemical speciation of copper in different color regions. The above information will be very useful in understanding the influence of copper element distribution and speciation on the color of porcelain.

2 Experimental section

The analyzed underglaze copper-red porcelain was made in the Yuan dynasty (AD 1271–1368) by Jingdezhen kiln. As shown in Fig. 1, the decoration shows red and black colors in some regions. For μ-XRF and μ-XANES analysis, a small piece including both red and black color was cut from the sample and the cross section was polished with silicon carbide paper to obtain a smooth plane. During the measurements, the cross sections in both red- and black-colored regions were scanned.

Both μ-XRF and μ-XANES measurements were performed at beamline BL15U1 at the Shanghai Synchrotron Radiation Facility (SSRF). SSRF is a third-generation synchrotron operating at a current of approximately 240 mA with top-up mode and energy of 3.5 GeV. The beamline BL15U1 at SSRF is an undulator beamline equipped with Si(111) double-crystal monochromator that has an energy resolution of 1.5 eV at 10 keV and Si(220) double-crystal monochromator that has an energy resolution of 0.5 eV at 10 keV. A K-B optics system is used to focus the monochromatized light into a width in the micrometer range. The sample stage consisted of multiple motor stages: two stages for scanning the sample in the horizontal and vertical directions and a third stage to align the sample into the image plane of the focusing device. The minimal step size of the motor stages was 20 nm [28].

During the μ-X-ray fluorescence mapping measurements, the intensity of the incoming X-ray was monitored using an ionization chamber, which was used for normalizing the measured X-ray intensity of the sample. X-ray fluorescence signals were detected using a single Vortex-90EX Si drift detector (SDD) from SII, USA, which provides excellent energy resolution and high output counting rate (< 136 eV @ 5.9 keV, at 100 kcps counting rate). The detector was placed at a 90° angle with respect to the incoming X-ray in order to decrease the intensity of the Compton scattering. The spot size at the sample location was 2 μm (H) × 2 μm (V) (FWHM). All the μ-XRF experiments were performed using monochromatic radiation at an exciting energy of 16 keV, and the test time was 1 s for every point. The μ-XRF data were analyzed using Igor Pro (software).

Cu speciation was assessed using XANES measurements. The absorption was measured while tuning the energy around the edge of the copper element (from 8929 to 9079 eV). The step size was 0.5 eV with the dwelling time of 1 s. The absorption was measured through the corresponding fluorescence emission, collected by the single Vortex-90EX Si drift detector. Energy calibrations were achieved using Cu foil as reference, and the position of the first inflection point was taken at 8979 eV. Copper

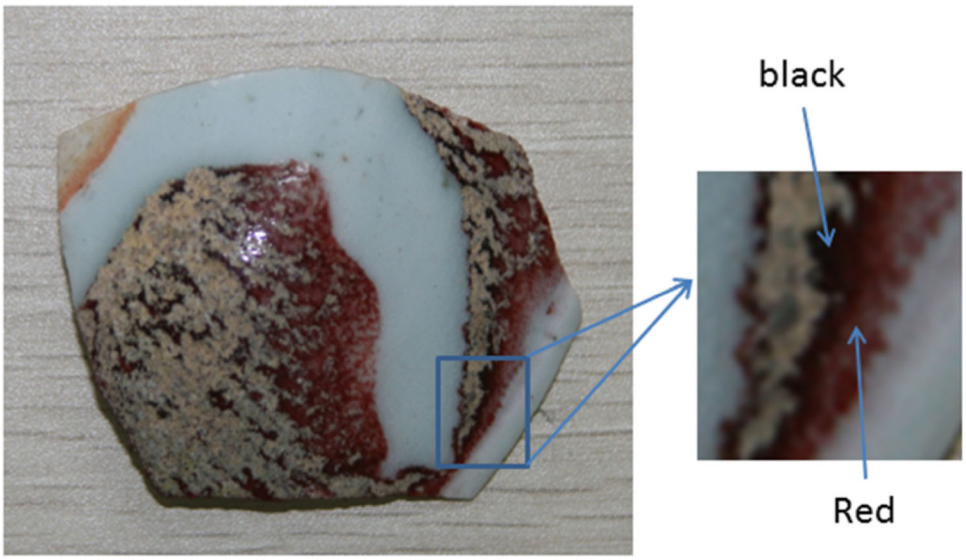

Fig. 1 (Color online) Underglaze copper-red porcelain analyzed in this study

metal, Cu_2O, and CuO were also measured as references. All XANES spectra were analyzed by using the Demeter software package [29].

3 Results and discussion

3.1 Distribution of elements in the cross section

XRF mapping was first performed on a cross section of red color region (mapped area: 450 μm (horizontal) × 550 μm (vertical)) (Fig. 2). Six elements, including Cu, Fe, Mn, Zn, Pb, and Rb, were detected in this area. Cu is mainly present in the glaze layer and shows a heterogeneous distribution. Fe and Mn have similar distributions in the glaze layer in that they are highly concentrated in some areas. Both Zn and Pb have relatively low content and are distributed rather homogeneously in the mapped area. Rb, as an element indicating the provenance of raw materials, has a higher content in the body than that in glaze. Furthermore, its content decreases gradually from body to the glaze surface.

To compare with distribution of elements in different color regions, an area of 400 μm (*H*) × 550 μm

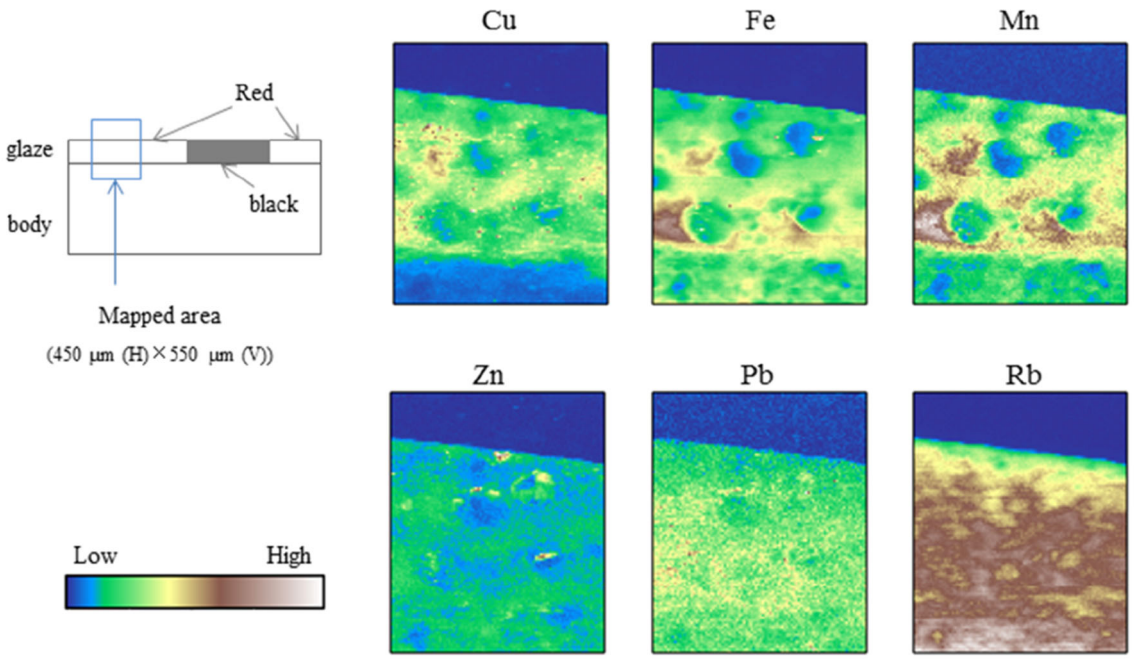

Fig. 2 (Color online) Elemental maps of red color region of underglaze copper-red porcelain

(*V*) covering the black-colored region was mapped (Fig. 3). A higher Cu content is present in the region of the interface between the glaze and body layers. Cu is mainly present in the glaze layer, and its concentration decreases gradually from body to the glaze surface. Similarly, patterned elemental distributions of Zn and Pb are also observed in this mapped area. Fe and Mn also show similar distribution because the two elements are part of the same group in the periodic table; thus, they have similar mass and physical characteristics. Rb is observed in both the glaze and body layers; the body layer contains the highest Rb content, a relatively high content in the glaze layer, and the lowest content in the glaze surface. A notable phenomenon is the absence of Rb in some areas having a high amount of Cu, Zn, and Pb in the interface between the glaze and body layers.

A boundary region of 1000 μm (*H*) × 440 μm (*V*) covering from black-colored region (left) to the red-colored region (right) was performed (Fig. S1) to better visualize the differences in distribution patterns between different regions. The content of Cu, Pb, and Zn is noticeably higher in the black-colored region than that in the red-colored region. As for Fe, Mn, and Rb, there is no difference in their content or distribution between different color regions. Similarly, patterned elemental distributions of Cu, Zn, and Pb, as well as similarly patterned elemental distributions of Fe and Mn, are also observed in the mapped area. To quantitatively investigate the elemental correlation between Cu, Pb, and Zn, the correlations between the XRF intensities of each element were extracted and plotted with the data in the selected interested regions shown in Fig. 4. Region of interests ROI 1 and ROI 2 are the boundary regions of the body and the glaze layers in the black-colored where the Cu was enriched. The correlation coefficients (*r*) of Cu versus Pb, Cu versus Zn, and Pb versus Zn are all greater than 0.84. These results also indicate a strong positive correlation among the distribution of Cu, Pb, and Zn in the black-colored region, whereas such phenomenon is not so prominent in the red-colored region (Fig. S2). A positive correlation is also found in ancient colored glass (both the red opaque glasses and blue transparent glasses) using copper as colorants [30–32].

According to the Chinese traditional decoration techniques of underglaze copper-red porcelain, the pigments are painted on the surface of the body first, then covered with transparent glaze, and fired at a kiln with strong reducing atmosphere. During the firing processes, pigments dissolved in the amorphous phase of the glaze and elements contained in pigments diffused from the high content region to the low content region. When the pigment layer is too thick to dissolve completely, the residual pigments could be found in the boundary region between the body and glaze of the porcelain [33]. Here, copper enriches in the interface region between the body and the glaze layers in the black-colored region, whereas it is distrusted irregularly in the red-colored region. Considering the indistinct boundary between the red-colored and the black-colored region, the enrichment of Cu, Zn, and Pb elements in the

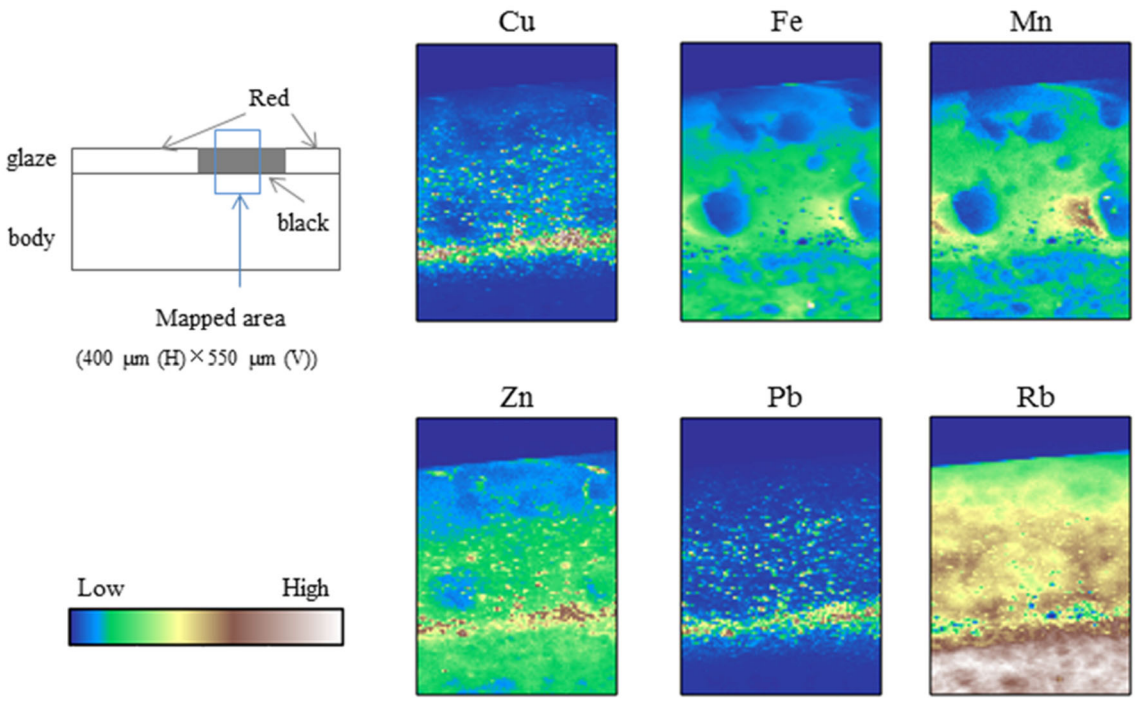

Fig. 3 (Color online) Elemental maps of the black-colored region of underglaze copper-red porcelain

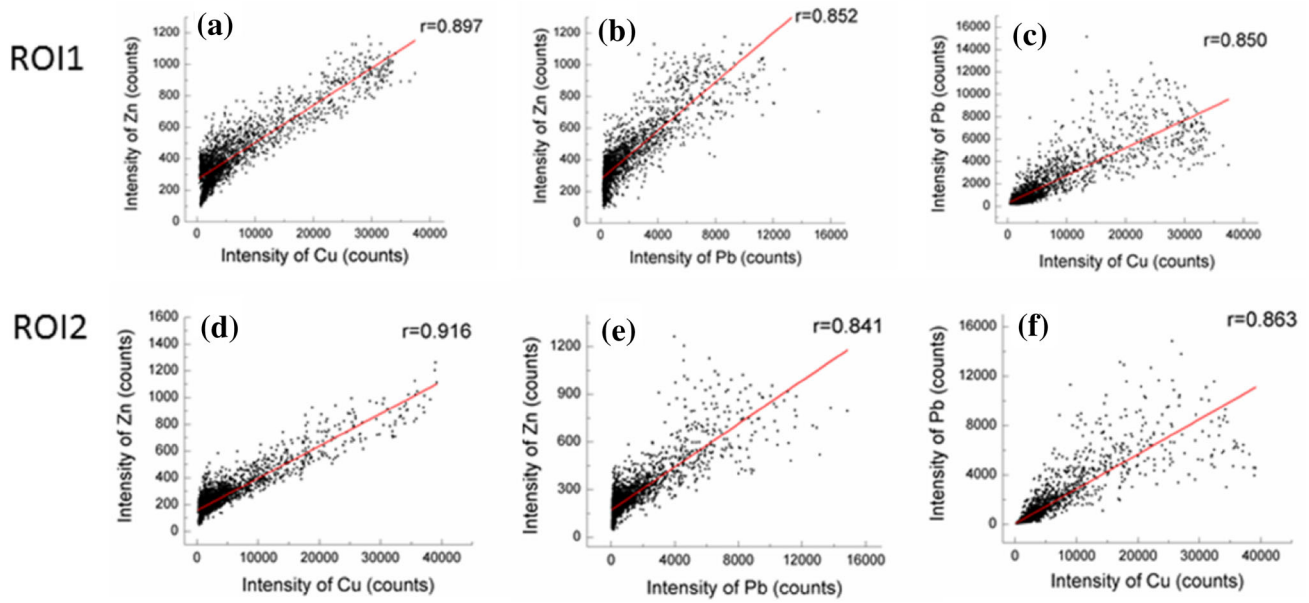

Fig. 4 Correlation between X-ray fluorescence intensities of Cu versus Pb, Cu versus Zn, and Pb versus Zn in the boundary regions between the body and glaze layers in black color where Cu enriched. *r* refers to the correlation coefficient

boundary region between the body and the glaze in the black-colored region may originate from the residual pigments. It is likely that the non-uniform thickness of the pigment layer is the reason that different distributions are observed in different color regions.

3.2 Cu K-edge XANES results

Micro-XANES spectra were recorded to obtain the Cu speciation contained in the cross section with different copper concentrations in the red- and black-colored region based on the pattern distributions. Figure 5a shows the Cu K-edge XANES spectra of three interested spots within the cross section of red-colored region. Here, spots A, B, and C correspond to areas with moderate Cu content, high Cu content, and low Cu content, respectively. The XANES spectra of the three spots showed a similar feature with a strong shoulder at 8983.6 eV. This confirmed the presence of Cu^{1+} in the red-colored region [34–37]. For spot B, two splits around 8995.4 eV and 9002.5 eV, and edge crest around 9024.7 eV in the post-edge region of the XANES spectrum as that of Cu foil indicate the existence of metallic copper particles. Because the concentration of Cu in the red region is relative low, the signal-to-noise ratio for other spots is too low to distinguish the Cu^0 features clearly.

Seven spots were selected in the black-colored region to obtain the Cu K-edge XANES spectra. The seven spots of interest were selected based on the following considerations: Spots A, B, and C denote the regions with the high Cu content, spots D and E denote the spots with moderate Cu content, and spots F and G denote the regions with the lowest Cu content. As shown in Fig. 5b, XANES spectra of spots A, B, and C refer to regions with similar features including a shoulder at 8981.7 eV and two split crests in post-edge region at 8993.6 eV and 9002.7 eV. These features are similar to that of Cu foil confirming the presence of metallic copper in spots A, B, and C [38]. For spots F and G, the XANES spectra also show the similar feature of the intense shoulder at 8983.7 eV. The post edge region could not be distinguished clearly as a result of the low signal-to-noise (SN) ratios. The strong shoulder at 8983.7 eV indicates the presence of monovalent copper ions. Comparatively, XANES spectra for spots D and E did not show prominent features that could be identified clearly. They have a weak shoulder around 8983 eV and the post-edge region with low SN ratios. Given that a strong shoulder usually means the presence of monovalent Cu ions and the absorption edge is near that of the Cu foil, the possible speciation in spots D and E is Cu^{1+} and metallic Cu.

Based on the above XANES results, Cu^{1+} and metallic Cu are present in different proportions, as indicated by red and black regions, respectively. Theoretically, Cu^{1+} ions in the glaze matrix are colorless. Thus, the origin of colors is related to copper metallic particles. According to Rayleigh scattering theory and the surface plasmon resonance peak, the absorption of copper particles in the visible range gives rise to a narrow peak at 570 nm, resulting in the red color from copper metallic particles. Furthermore, the plasmon peak wavelength is closely related to the particle size, inter-particle distances, and electronic coupling, among

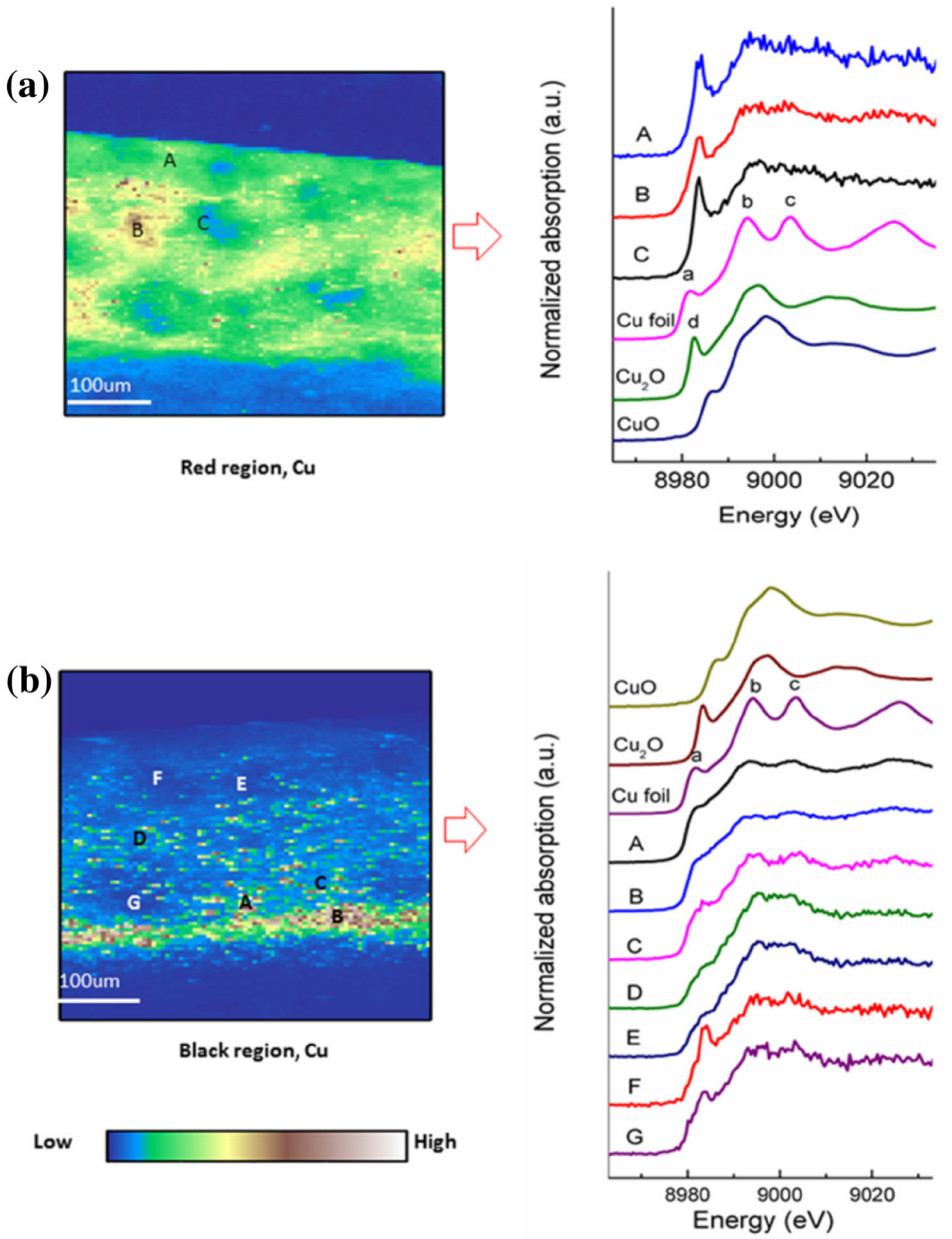

Fig. 5 (Color online) Cu K-edge XANES spectra taken at spots of interest in red and black color regions

others [7–9, 38]. Here, the spot size of X-ray is 2 um for all interested spots measurements. For spots A, B, and C in the black region, only the features of metallic copper are observed. However, for spots in the red region, Cu^{1+}, and possibly Cu^{0}, exists in the same measured area. This indicates that the different sizes of copper particles are likely the reason for different colors.

Another question that needs to be asked is why Cu speciation is different as both red and black colors are fired simultaneously under the same firing atmosphere. There are two possible reasons for this: The first one is with regard to the Cu content. On extracting the XRF intensity of interested spots of Cu, Zn, and Pb elements (Table S1), the Cu content for spots A, B, and C in the black region is observed to be much larger than other interested spots. Even for the red region, the Cu content for spot B is larger than that for spots A and C. The second reason is related to the existence of Zn and Pb [7–9]. As shown in Fig. S1, the distribution of Zn and Pb shows an obvious difference compared with that of Fe and Mn. Both Zn and Pb demonstrate a larger metal activity than Cu. Thus, the existence of these elements could promote the formation of metallic copper particles.

4 Conclusion

The combination of μ-XRF and μ-XANES analysis at a micrometer resolution has been employed to investigate the spatial distribution and chemical speciation of copper contained in red and black regions, respectively, of the underglaze copper-red porcelain glaze layer. The difference in the distribution pattern and chemical speciation of Cu are observed in different color regions. In the black region, copper is enriched in the interface region between the body and glaze layers and metallic copper particles are the main speciation. The distribution of Pb and Zn presents a high positive correlation with that of Cu in the black region. On the contrary, the distribution of Cu is irregular in the red region with multi-valence speciation and demonstrates no positive correlation with Pb and Zn for fusion at high temperatures. This confirms the influence of Cu speciation on the color of Chinese underglaze copper-red porcelain. Furthermore, although this study is only a preliminary work, it did clearly show that the combination of μ-XRF and μ-XANES could provide more fundamental information useful for understanding the influence of Cu on the color of underglaze copper-red porcelain. In future research, a larger set of Chinese copper-red porcelain as well as more reference materials will be considered to deepen the understanding of such underglaze techniques.

Acknowledgements We appreciate the BL15U1 beamline at Shanghai Synchrotron Radiation Facility for providing the beamtime to carry out the μ-XRF and μ-XANES experiments.

References

1. J.Z. Li, *History of Science and Technology of China (Ceramic Volume)* (Science Press, Beijing, 1998)
2. J.W. Mellor, Chemistry of Chinese copper-red glazes. Trans. Ceram. Soc. **35**(8), 364–378 (1936)
3. R.F. Huang, X.Q. Chen, S.P. Chen et al., Submicroscopic structure of copper red glaze in Ming and Qing dynasties. China Ceram. **03**, 58–62 (1986)
4. P.A. Cuvelier, C. Andraud, D. Chaudanson et al., Copper red glazes: a coating with two families of particles. Appl. Phys. A Mater. **106**(4), 915–929 (2012). https://doi.org/10.1007/s00339-011-6707-3
5. W. Klysubun, Y. Thongkam, S. Pongkrapan et al., XAS study on copper red in ancient glass beads from Thailand. Anal. Bioanal. Chem. **399**(9), 3033–3040 (2011). https://doi.org/10.1007/s00216-010-4219-1
6. C. Maurizio, F. d'Acapito, M. Benfatto et al., Local coordination geometry around Cu^{+} and Cu^{2+} ions in silicate glasses: an X-ray absorption near edge structure investigation. Eur. Phys. J. B **14**, 211–216 (2000). https://doi.org/10.1007/s100510050122
7. P. Colomban, A. Tournié, P. Ricciardi, Raman spectroscopy of copper nanoparticle-containing glass matrices: ancient red stained-glass windows. J. Raman Spectrosc. **40**, 1949–1955 (2009). https://doi.org/10.1002/jrs.2345
8. Ph Sciau, L. Noé, Ph Colomban, Metal nanoparticles in contemporary potters' master pieces: lustre and red "pigeon blood" potteries as models to understand the ancient pottery. Ceram. Int. **42**, 15349–15357 (2016). https://doi.org/10.1016/j.ceramint.2016.06.179
9. Ph Colomban, The use of metal nanoparticles to produce yellow, red and iridescent colour, from bronze age to present times in lustre pottery and glass: solid state chemistry, spectroscopy and nanostructure. J. Nano Res. **8**, 109–132 (2009). https://doi.org/10.4028/www.scientific.net/JNanoR.8.109
10. W.D. Kingery, P.B. Vandiver, *An Islamic Lusterware from Kashan, Ceramic Masterpieces* (The Free Press, New York, 1986), pp. 111–121
11. A. Ram, S.N. Prasad, Mechanism of formation of color in copper red glass, in *Advances in Glass Technology, Part I* (Plenum Press, New York, 1962), pp. 256–269
12. S. Banerjee, A. Paul, Thermodynamics of the system Cu–O and ruby formation in borate glass. J. Am. Ceram. Soc. **57**, 286–290 (1974). https://doi.org/10.1111/j.1151-2916.1974.tb10902.x
13. M. Wakamatsu, N. Takeuchi, S. Ishida, Effect of heating and cooling atmosphere on colors of glaze and glass containing copper. J. Non Cryst. Solids **80**, 412–421 (1986). https://doi.org/10.1016/0022-3093(86)90425-4
14. M. Wakamatsu, N. Takeuchi, H. Nagai et al., Chemical states of copper and tin in copper glazes fired under various atmosphere. J. Am. Ceram. Soc. **72**, 16–19 (1989). https://doi.org/10.1111/j.1151-2916.1989.tb05946.x
15. L. Guan, J. Zhu, C.S. Fan, Y.M. Yang et al., Micro SR-XRF analysis on underglaze copper red porcelain of Ming dynasty. Nucl. Tech. **36**(7), 070103 (2013). **(in Chinese)**
16. J. Zhu, H.P. Duan, Y.M. Yang et al., Colouration mechanism of underglaze copper-red decoration porcelain (AD 13th–14th century), China. J. Synchrotron Radiat. **21**, 751–755 (2014). https://doi.org/10.1107/S1600577514009382
17. C. Lu, J.X. Jiang, C.Q. Xu et al., Coloration mechanism of Xuande sacrificial red porcelain from Guan kiln of Jingdezhen in China. J. Univ. Chin. Acad. Sci. **33**(3), 421–426 (2016). https://doi.org/10.7523/j.issn.2095-6134.2016.03.020
18. M.C.C. Pinzani, A. Somogyi, A.S. Simionovici et al., Direct determination of cadmium speciation in municipal solid waste fly ashes by synchrotron radiation induced μ-X-ray fluorescence and μ-X-ray absorption spectroscopy. Environ. Sci. Technol. **36**, 3165 (2002). https://doi.org/10.1021/es010261o
19. L. Vincze, A. Somogyi, J. Osán et al., Quantitative trace element analysis of individual fly ash particles by means of X-ray microfluorescence. Anal. Chem. **74**, 1128 (2002). https://doi.org/10.1021/ac010789b
20. M.C. Camerani, A. Somogyi, B. Vekemans et al., Determination of the Cd-bearing phases in municipal solid waste and biomass single fly ash particles using SR-μXRF spectroscopy. Anal. Chem. **79**, 6496 (2007). https://doi.org/10.1021/ac070206j
21. L.H. Wang, X.M. Lu, Y.Y. Huang, Determination of Zn distribution and speciation in basic oxygen furnace sludge by synchrotron radiation induced μ-XRF and μ-XANES microspectroscopy. X Ray Spectrom. **42**, 423–428 (2013). https://doi.org/10.1002/xrs.2494
22. M. Zi, X. Wei, H. Yu et al., Stratified structure in ancient paints studied by synchrotron confocal micro-X-ray method. Nucl. Tech. **38**, 060101 (2015). https://doi.org/10.11889/j.0253-3219.2015.hjs.38.060101. **(in Chinese)**
23. M. Shang, T. Zhao, H. Bao et al., In situ XAFS characterization of bimetallic nanoparticle catalysts PtCo/C structure changes in the working conditions. Nucl. Tech. **39**, 060101 (2016). https://doi.org/10.11889/j.0253-3219.2016.hjs.39.060101. **(in Chinese)**
24. G.L. Chang, D.G. Wang, Y.Y. Zhang et al., ALD-coated ultrathin Al_2O_3 film on BiVO4 nanoparticles for efficient PEC water

splitting. Nucl. Sci. Tech. **27**, 108 (2016). https://doi.org/10.1007/s41365-016-0122-6
25. Y.Y. Yang, Q. Sao, S.-Q. Gu et al., Soller slits automatic focusing method for multi-element fluorescence detector. Nucl. Sci. Tech. **27**(5), 115 (2016). https://doi.org/10.1007/s41365-016-0105-7
26. P.Q. Duan, H.L. Bao, J. Li et al., In-situ high-energy-resolution X-ray absorption spectroscopy for UO_2 oxidation at SSRF. Nucl. Sci. Tech. **28**, 2 (2017). https://doi.org/10.1007/s41365-016-0155-x
27. X.P. Sun, F.F. Sun, S.Q. Gu et al., Local structural evolutions of $CuO/ZnO/Al_2O_3$ catalyst for methanol synthesis under operando conditions studied by in situ quick X-ray absorption spectroscopy. Nucl. Sci. Tech. **28**, 21 (2017). https://doi.org/10.1007/s41365-016-0170-y
28. L.L. Zhang, S. Yan, S. Jiang et al., Hard X-ray micro-focusing beamline at SSRF. Nucl. Sci. Tech. **26**(6), 060101 (2015). https://doi.org/10.13538/j.1001-8042/nst.26.060101
29. Demeter: XAS Data Processing and Analysis. http://bruceravel.github.io/demeter/. Accessed 24 Apr 2019
30. A.N. Shugar, Byzantine opaque red glass tesserae from Beit Shean, Israel. Archaeometry **42**(2), 375–384 (2000). https://doi.org/10.1111/j.1475-4754.2000.tb00888.x
31. A. Santagostino Barbone, E. Gliozzo, F. D'Acapito et al., The SECTILIA panels of Faragola (ASCOLI SATRIANO, SOUTHERN Italy): a multi-analytical study of the red, orange and yellow glass slabs. Archaeometry **50**(3), 451–473 (2008). https://doi.org/10.1111/j.1475-4754.2007.00341.x
32. R.H. Brill, N.D. Cahill, A red opaque glass from Sardis and some thoughts on red opaques in general. J. Glass Stud. **30**, 16–27 (1988)
33. F.K. Zhang, Study on Changsha ware. J. Chin. Ceram. Soc. **14**(3), 339–348 (1986). **(in Chinese)**
34. S. Quartieri, R. Arletti, Chapter 4.3, in *The use of X-Ray Absorption Spectroscopy in Historical Glass Research, Modern Methods for analyzing Archaeological and Historical Glass*, 1st edn., ed. by K. Janssens (Wiley, Hoboken, 2013)
35. A. Silvestri, S. Tonietto, F. D'Acapito et al., The role of copper on colour palaeo-Christian glass mosaic tesserae: an XAS study. J. Cult. Herit. **13**, 137–144 (2012). https://doi.org/10.1016/j.culher.2011.08.002
36. S. Padovani, C. Sada, P. Mazzoldi et al., Copper in glazes of Renaissance luster pottery: nanoparticles, ions, and local environment. J. Appl. Phys. **93**(12), 10058–10063 (2003). https://doi.org/10.1063/1.1571965
37. G. Chen, S.Q. Chu, T.X. Sun et al., Confocal depth-resolved fluorescence micro-X-ray absorption spectroscopy for the study of cultural heritage materials: a new mobile endstation at the Beijing Synchrotron Radiation Facility. J. Synchrotron Radiat. **24**, 1000–1005 (2017). https://doi.org/10.1107/S1600577517010207
38. I. Nakai, C. Numako, H. Hosono et al., Origin of the red color of Satsuma copper-ruby glass as determined by EXAFS and optical absorption spectroscopy. J. Am. Ceram. Soc. **82**(3), 689–695 (1999). https://doi.org/10.1111/j.1151-2916.1999.tb01818.x